# Effective optical constants in stratified metal–dielectric metameterial

**Masanobu Iwanaga**

*Department of Physics, Graduate School of Science, Tohoku University, Sendai 980-8578, Japan*

Received January 2, 2007; revised February 8, 2007; accepted February 25, 2007;
posted February 26, 2007 (Doc. ID 78547); published April 17, 2007

Effective optical constants of stratified metal–dielectric metameterial are presented. The effective constants are determined by the two-complex reflectivity method (TCRM). The TCRM reveals the full components of the effective permittivity and permeability tensors and indicates the remarkable anisotropy of metallic and dielectric components below the effective plasma frequency. On the other hand, above the plasma frequency, one of the effective refractive indices takes a positive value less than unity and is associated with small loss. The photonic states are confirmed by the distribution of electromagnetic fields. © 2007 Optical Society of America

*OCIS codes:* 000.4430, 160.4760, 260.2130, 260.5740.

Photonic metamaterials attract great interest as a new type of material including magnetic resonance at optical frequency. A famous example exploiting magnetic resonance is negative refraction.[1]

Evaluation of effective optical constants at optical frequency has been performed for metamaterials of thin layers.[2] In analyzing bulk metamaterials, reflective polarimetry is the only way to obtain effective optical constants. It is necessary in the analysis to satisfy the equation of dispersion. This Letter presents a way of analysis, the two-complex reflectivity method (TCRM), to determine the full components of the effective tensors of permittivity $\epsilon$ and permeability $\mu$. Moreover, the photonic states implied by the effective optical constants are examined.

Figure 1 shows a stratified metal–dielectric metamaterial (SMDM) and coordinate system. The composite material is obviously uniaxial, and the $z$ axis is set parallel to the optical axis. Here we set the metal to be Ag and the dielectrics to be $MgF_2$. The pair of constituents is selected to reduce loss in materials and the interfaces.[3]

We assume that effective tensors $\epsilon$ and $\mu$ are diagonal and describe the local response in media. The principal axes of both tensors are set to be the $x$, $y$, and $z$ axes in Fig. 1(a). In the configuration shown in Fig. 1(b), incident light is $s$ polarized (that is, $\mathbf{E}_{\text{in}} \| y$), and the following relation is derived from the Maxwell boundary conditions concerning bulk material in vacuum ($n_1=1$, $\epsilon_1=1$, and $\mu_1=1$):

$$\frac{\hat{k}_z(\theta)}{\mu_x} = \frac{n_1 \cos\theta}{\mu_1} \cdot \frac{1 - r_s(\theta)}{1 + r_s(\theta)}. \tag{1}$$

We set $\mathbf{E}(r,t) \propto \exp(i\mathbf{k}\cdot\mathbf{r} - i\omega t)$ and $\hat{\mathbf{k}} = \mathbf{k}/k_0$, where $k_0$ is the wavenumber of light in vacuum. The component $\hat{k}_z$ represents the refraction; in particular, $\hat{k}_z(0)$ is the refractive index along the $z$ axis. Complex reflectivity $r_s$ was obtained by numerical calculation based on the scattering-matrix method,[4] improved in numerical convergence.[5] Optical constants of Ag were taken from literature,[6] and the refractive index of $MgF_2$ was set at 1.38.

The equation of dispersion under $s$ polarization is

$$\epsilon_y = \frac{\hat{k}_z(\theta)^2}{\mu_x} + \frac{\hat{k}_x(\theta)^2}{\mu_z}, \tag{2}$$

where $\hat{k}_x(\theta) = n_1 \sin\theta$.

After substituting Eq. (1) for Eq. (2), two different angles make it possible to evaluate $\epsilon_y/\mu_x$ and $\mu_x\mu_z$ uniquely. The products of $\epsilon_z/\mu_y$ and $\mu_y\mu_x$ are obtained by permutating configuration $(x,y,z) \to (y,z,x)$. In uniaxial media of $\epsilon_x = \epsilon_y$ and $\mu_x = \mu_y$, only the two configurations are enough to determine all the values of tensors of $\epsilon$ and $\mu$ except for the sign. We call this procedure the TCRM. This method is a generalization of the two-reflectance method (TRM),[7,8] which is

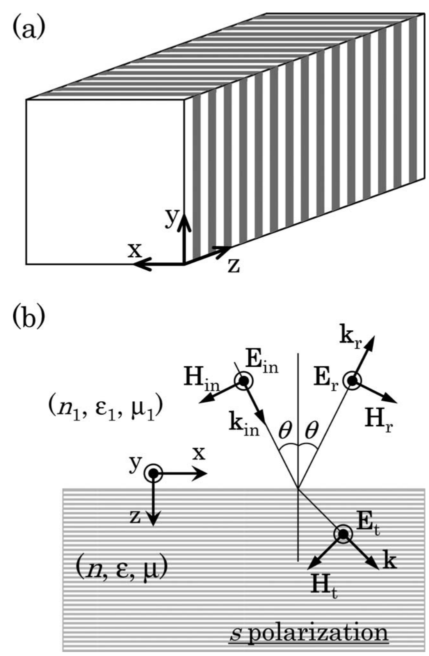


Fig. 1. (a) Schematic drawing of SMDM and the coordinate configuration. Gray indicates metal (silver) layers, and white is dielectric ($MgF_2$) layers. (b) Optical configuration of the TCRM. Incident light is $s$ polarization, that is, $\mathbf{E}_{\text{in}} \| y$.

0146-9592/07/101314-3/$15.00 

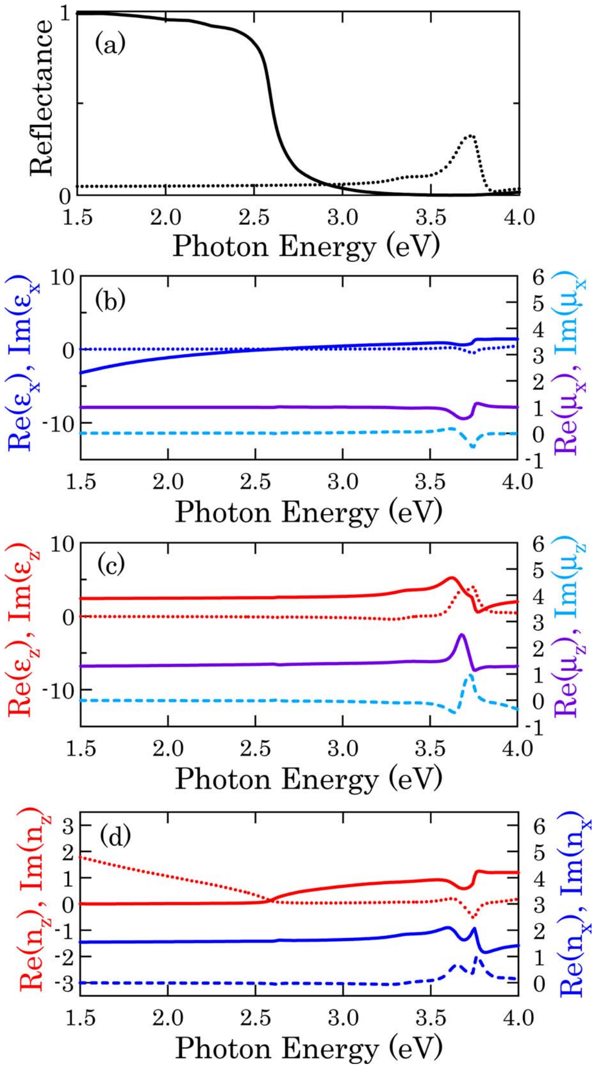


Fig. 2. (Color online) (a) Reflectance spectra. Solid line, under normal incidence on the $xy$ plane; dotted line, under nornal incidence with $\mathbf{E}_{\mathrm{in}} \| z$ on the $yz$ plane. (b) $x$ component of effective $\epsilon$ and $\mu$. Upper solid line, $\mathrm{Re}(\epsilon_x)$; dotted line, $\mathrm{Im}(\epsilon_x)$; lower solid line, $\mathrm{Re}(\mu_x)$; dashed line, $\mathrm{Im}(\mu_x)$. (c) $z$ component of effective $\epsilon$ and $\mu$. The notations are similar to (b): replace $x$ in (b) with $z$. (d) Refractive indices. Upper solid line, $\mathrm{Re}(n_z)$; dotted line, $\mathrm{Im}(n_z)$; lower solid line, $\mathrm{Re}(n_x)$; dashed line, $\mathrm{Im}(n_x)$.

valid for materials of $\mu=1$. In TRM, conformal mapping between reflectance at two incident angles plays a crucial role and retrieves the phase of complex reflectivity. On the other hand, if it is assumed that $\mu \neq 1$, we need two-complex reflectivity to evaluate the $\epsilon$ and $\mu$ tensors. Thus, although the TCRM stems from the TRM, the formalism is quite different.

It is nontrivial how to determine the sign of $\mu_x$. Actually we take the sign to satisfy $\mu_x \approx 1$ at off-resonance energy of 1.5 eV and to connect $\mu_x$ at resonance without a discontinuous jump. Once the sign of $\mu_x$ is identified, other components of $\mu_z$, $\epsilon_x$, and $\epsilon_z$ are evaluated uniquely; the refractive component $\hat{k}_z$ is also evaluated uniquely by use of Eq. (1). As shown in Fig. 2, this way determines effective tensors $\epsilon$ and $\mu$ in a wide energy range.

Figure 2(a) shows the reflectance spectra in the two configurations for the TCRM; the solid line indicates the reflectance spectrum under normal incidence on the $xy$ plane, and the dotted line shows the spectra under normal incidence with $\mathbf{E}_{\mathrm{in}} \| z$ on the $yz$ plane. The periodicity of SMDM is 75 nm, and the thicknesses of Ag and $MgF_2$ are 15 and 60 nm, respectively. The surface layer parallel to the $xy$ plane is set to be $MgF_2$, and the thickness is set to be 30 nm. The reflectance spectrum shown by the solid line was evaluated for thick SMDM of 2000 periods in numerical evaluation, and the reflectance shown by the dotted line was calculated for 50 mm thick SMDM. The thickness is enough to ensure that the two reflectances (and $r_s$) are numerically the same with infinitely thick SMDM. The numerical accuracy is tested by changing the number of Fourier harmonics employed in the numerical calculation for $r_s$ and is estimated within a few percent.

Figures 2(b) and 2(c) display the $x$- and $z$-components of the effective $\epsilon$ and $\mu$, respectively. In Figs. 2(b) and 2(c), the upper solid lines denote $\mathrm{Re}(\epsilon_i)$ and the lower solid lines stand for $\mathrm{Re}(\mu_i)$ $(i=x,z)$. In this TCRM analysis, two angles of 0° and 15° are employed. Other pairs of angles yield same results within the numerical errors. It is therefore confirmed that TCRM determines the full components of $\epsilon$ and $\mu$ with the satisfying equation of dispersion in SMDM. The component $\epsilon_x$ represents typical permittivity of Drude metal below 3.5 eV. The effective plasma frequency $\omega_{\mathrm{p,eff}}$ is located at $\hbar\omega_{\mathrm{p,eff}}=2.6$ eV. On the other hand, $\epsilon_z$ implies that SMDM is dielectric for the light of $\mathbf{E} \| z$. Below 3.5 eV there exists no prominent magnetic resonance in SMDM, whereas magnetic resonance appears at 3.7 eV. The resonance deviates from simple Lorentzian dispersion and is associated with resonant behavior of permittivity. The 3.7 eV resonance is thus a mixed one of electromagnetic (EM) components and shows a complex response due to the anisotropy of SMDM. This resonant behavior is discussed below in more detail.

Figure 2(d) presents effective refractive indices. SMDM shows a metallic color similar to gold when seen from the $xy$ plane, whereas it is a transparent dielectric material of refractive index 1.8 in the visible range for the light of $\mathbf{E} \| z$ in the $yz$ or $xz$ planes.

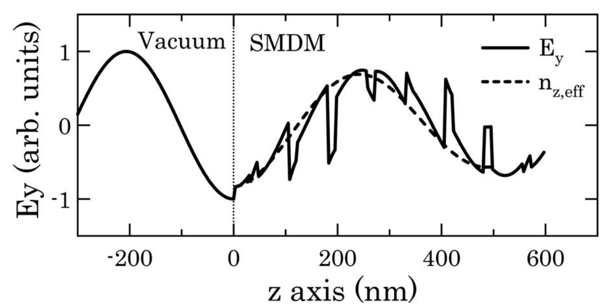


Fig. 3. (a) Effect of refractive index $n_z$ at 3.0 eV. Solid line, electric field $E_y(z)$ of the incident light ($\mathbf{E}_{\mathrm{in}} \| y$, normal incidence on the $xy$ plane) in vacuum and the refracted component in SMDM; dashed line, $E_y(z)$ evaluated by using $n_z$; Fig. 2(d) shows $n_z=0.67+0.04i$ at 3.0 eV.

In particular, loss in SMDM is quite suppressed in the wide range of 2.6–3.5 eV. This is a feature of SMDM. Although the permittivity of bulk Ag implies a large loss in the energy range, the composite of Ag and $MgF_2$ is nearly free from loss. This result suggests that EM fields in metallic layers help make transmission highly efficient; that is, it suggests that there exists EM-field enhancement. Indeed, above $\omega_{p,eff}$, several layers of metal and dielectrics show high transmittance.[9] Figure 2(d) indicates that highly efficient transmission in SMDM is associated with an effective refractive index $n_z$ of $0<\mathrm{Re}(n_z)<1$. The effective index thus provides a concise description for the photonic state. Next, we examine the EM-field distribution in SMDM to clarify whether the state is actually realized.

Figure 3 displays the $E_y$ profile along the $z$ axis at 3.0 eV. Incident light travels along the $z$ axis and illuminates the $yz$ plane with $\mathbf{E}_{in} \| y$. The solid line shows incident light in vacuum and the refracted component in SMDM. In this configuration the effective refractive index is $n_z=0.67+0.04i$ from Fig. 2(d). The $E_y$ reproduced by $n_z$ is shown by the dashed line. The wavelength in SMDM is obviously close to $\lambda/\mathrm{Re}(n_z)$ and longer than $\lambda$ ($\lambda$ is the wavelength in vacuum). Consequently, it is definitely confirmed that the effective description for SMDM works well. In particular, the effective description is in excellent agreement within a $\lambda/\{4\mathrm{Re}(n_z)\}$ scale from the interface and suggests that the TCRM mainly analyzes the EM responses within the $\lambda/\{4\mathrm{Re}(n_z)\}$ depth. The index $n_z$ represents the low-loss photonic state in a wide range of 2.6–3.5 eV, where the phase velocity exceeds the velocity of light $c$ in vacuum. Figure 3 also shows that the EM wave in SMDM is not the ideal plane wave and is affected by periodic structure. This is one of the inevitable properties in mesoscopic metamaterial optics.

The end of this discussion refers to the unusual behavior of $\mathrm{Im}(n_z)$ at 3.7 eV in Fig. 2(d). At resonance, $\mathrm{Im}(n_z)$ takes a negative value and seems to imply an exponentially growing wave. However, as shown in Fig. 4, the EM distribution at 3.7 eV (solid line) does not show any such growing wave and indicates EM-field enhancement in metallic layers. The index $n_z$ implies the profile shown by the dashed line in Fig. 4 and roughly reproduces the EM fields in SMDM within a half-wavelength scale from the interface.

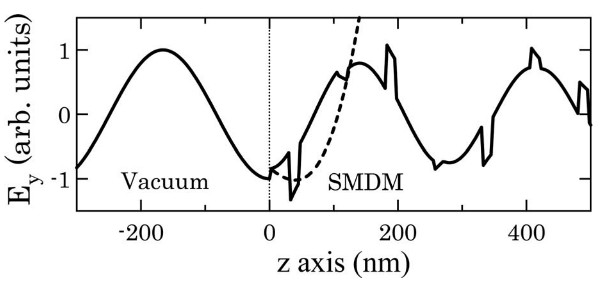


Fig. 4. Profile of electric field $E_y$ at 3.74 eV (solid line) under normal incidence on the $xy$ plane. Dashed line, profile calculated from the effective refractive index $n_z$ at 3.74 eV in Fig. 2(d). Weak reflection is not included in vacuum for simplicity.

Why does such unusual behavior appear? In Fig. 4, the wavelength in vacuum is $\lambda=331$ nm and the periodicity of SMDM is 75 nm. It therefore still seems possible to use the effective description; however, the other component is $\mathrm{Re}(n_x)=2.0$ and $\lambda/\mathrm{Re}(n_x)=166$ nm, which is about twice the periodicity. The condition in Fig. 4 is likely close to limits of effective description. Additionally we note that the limits of effective description in the GHz range were eagerly debated[10–13]; one of the limits is at present understood to be $\lambda/|\mathrm{Re}(n_{eff})| \sim$ periodicity.

From the numerical results and discussion, we can extract a few lessons for TCRM analysis: (i) For wavelength $\lambda$ in vacuum and periodicity $a$ in metamaterial, it is at least necessary that $\lambda/|\mathrm{Re}(n_{eff})|>2a$, to obtain the usual effective refractive index, $\mathrm{Im}(n_{eff})\geqslant 0$. This condition is satisfied below 3.5 eV in Fig. 2, and both $\epsilon$ and $\mu$ are determined successfully. (ii) Effective optical constants are determined by the optical response mainly within a $\lambda/|4\mathrm{Re}(n_{eff})|$ scale from the interface.

In conclusion, the scheme of a two-complex reflectivity method has been presented, this TCRM has been applied to stratified metal–dielectric metamaterial, and the full components of $\epsilon$ and $\mu$ have been revealed. Analysis of EM distribution has confirmed that the effective refractive index describes the photonic states in SMDM below 3.5 eV well. The effective index indicates that the low-loss photonic states with phase velocity larger than $c$ exists in a wide energy range above $\omega_{p,eff}$.

The author (M.Iwanaga@osa.org) thanks T. Ishihara for discussion and comments on the manuscript. This study is partially supported by the Research Foundation for Opto-Science and Technology and by the Information Synergy Center, Tohoku University, who assisted in numerical implementation.

## References

1. J. B. Pendry and D. R. Smith, Phys. Today **57**(6), 37 (2004).
2. D. R. Smith, S. Schultz, P. Markoš, and C. M. Soukoulis, Phys. Rev. B **65**, 195401 (2002).
3. G. Dolling, C. Enkrich, M. Wegener, C. M. Soukoulis, and S. Linden, Opt. Lett. **31**, 1800 (2006).
4. S. G. Tikhodeev, A. L. Yablonskii, E. A. Muljarov, N. A. Gippius, and T. Ishihara, Phys. Rev. B **66**, 045102 (2002).
5. L. Li, J. Opt. Soc. Am. A **13**, 1870 (1996).
6. P. B. Johnson and R. W. Christy, Phys. Rev. B **6**, 4370 (1972).
7. R. M. A. Azzam, J. Opt. Soc. Am. **69**, 590 (1979).
8. R. M. A. Azzam, Appl. Opt. **19**, 3361 (1980).
9. M. Scalora, M. J. Blemer, A. S. Manka, S. D. Pethel, J. P. Dowling, and C. M. Bowden, J. Appl. Phys. **83**, 2377 (1998).
10. T. Koschny, P. Markoš, D. R. Smith, and C. M. Soukoulis, Phys. Rev. E **68**, 065602(R) (2003).
11. T. Koschny, P. Markoš, D. R. Smith, and C. M. Soukoulis, Phys. Rev. E **70**, 048603 (2004).
12. R. A. Depine and A. Lakhtakia, Phys. Rev. E **70**, 048601 (2004).
13. A. L. Efros, Phys. Rev. E **70**, 048602 (2004).